

Electrical conduction and transmission electron microscopy studies of CdSe_{0.8}Te_{0.2} thin films

P. J. SEBASTIAN, V. SIVARAMAKRISHAN

Thin Film Laboratory, Department of Physics, Indian Institute of Technology, Madras-600 036, India

Electrical resistance of CdSe_{0.8}Te_{0.2} thin films were found to be dependent on various film parameters such as substrate temperature, film thickness, deposition rate and post-deposition heat treatment in different environments. A decrease in film resistivity was observed for thicker films and for those heat treated in vacuum. Films deposited at higher substrate temperatures and faster rates showed an increase in film resistivity. A spectrum of activation energies was observed in the films which fell within either of the activation energies observed in CdSe or CdTe films. Films heated in an oxygen environment showed an increase in film resistivity with a different activation energy. Transmission electron microscopy (TEM) of the films showed an improvement in crystallinity with increasing film thickness and substrate temperature, and a reduction in crystallinity with increasing deposition rate.

1. Introduction

CdSe_xTe_{1-x} thin films are very useful in semiconductor technology. They are used in devices such as solar cells [1], photoconductors [2], thin film transistors [3], etc. Other applications include vidicons, photo-detectors and IR detectors. However the film resistivity has been found to depend on various parameters such as film thickness, substrate temperature, post-deposition heat treatment, deposition rate, ambient gas, etc. Unless one has sufficient control over these parameters, to achieve stable and films with reproducible results is very difficult. We have succeeded in controlling these parameters to obtain reproducible results for the films.

Earlier studies [4–13] on this system have mainly given attention to the characterization and composition dependence of film conductivity, and to the Hall effect. But no selective study has been reported for this material.

We have chosen a single composition, CdSe_{0.8}Te_{0.2}, from the pseudobinary CdSe_xTe_{1-x} to study the electrical conduction mechanism and the various parameters which control it. In this work we have tried to correlate the various film and growth parameters with film resistance. Transmission electron microscopy (TEM) studies were performed on films for structural characterization as well as to study the grain size variation with film thickness, deposition rate and substrate temperature. All the measurements were carried out in the temperature range 300–400 K.

2. Experimental procedure

Bulk samples were prepared from pure CdSe and CdTe by vacuum sealing followed by heating in a furnace at 950 °C for 24 h and subsequent quenching in water.

Well-cleaned thin glass substrates were used for deposition of the film. An ultrasonic cleaner was used for cleaning the glass substrates. For evaporation of the bulk material, a conventional resistive heating technique was used. Glass substrates were kept at about 20 cm above the source. Film resistance was measured using a Keithley 610 C electrometer connected to precoated indium contacts by thin copper leads. Film thickness and deposition rate were monitored using a quartz crystal thickness monitor. Film temperature (substrate temperature) was measured using a copper–constantan thermocouple. Structural analysis was carried out using an X-ray diffractometer, and electron probe micro analysis (EPMA) was used for composition analysis. The transmission electron micrographs and diffractograms were taken with a Philips scanning transmission electron microscope CM-12. Deposition, as well as *in situ* measurements, was carried out at a pressure lower than 10⁻⁵ torr.

3. Results and discussion

X-ray and electron diffraction studies of the films showed that CdSe_{0.8}Te_{0.2} thin films are polycrystalline with hexagonal (wurtzite) type crystals. This result agrees with the literature. Heating and cooling cycles were carried out on as-deposited films in vacuum as well as in an oxygen environment. Film resistance was monitored during heating and cooling cycles. Films were heated between 300 and 400 K, at a rate of 1 K min⁻¹.

Fig. 1 shows $\ln(R)$ against $1/T$ plotted for films of two different thicknesses in vacuum and in oxygen, where R is the film resistance in Ω and T is the substrate temperature in Kelvin. The solid lines 1–3 give the first heating in vacuum, subsequent heating/cooling in vacuum and heating in oxygen, respectively,

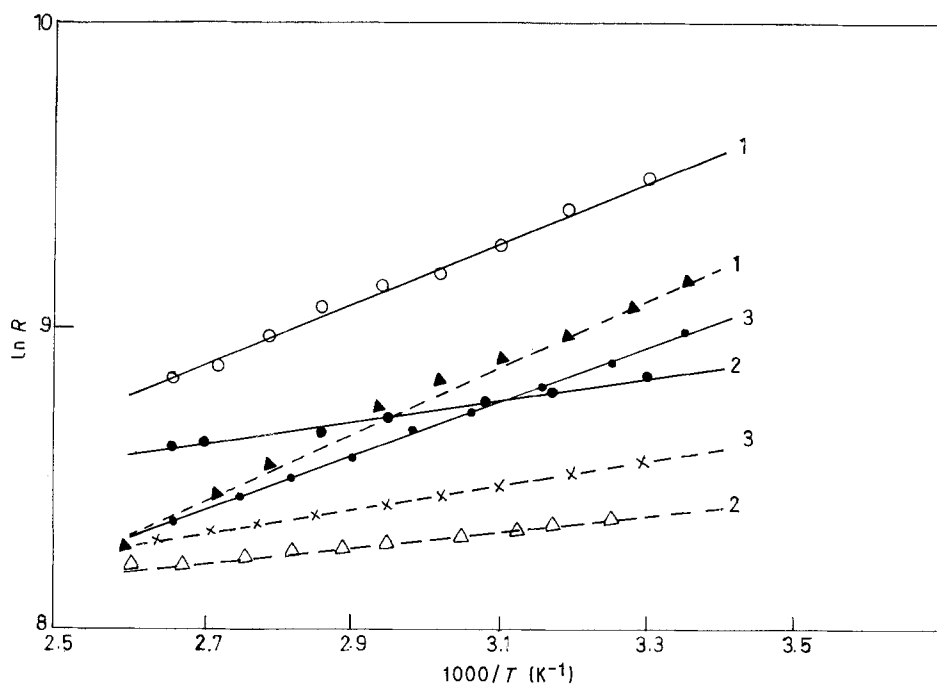


Figure 1 $\ln(R)$ against $1/T$ for films of thickness 80 nm: solid lines 1, first heating in vacuum; 2, subsequent heating/cooling in vacuum; 3, heating in oxygen; and 100 nm: dashed lines —1, first heating in vacuum; 2, subsequent heating/cooling in vacuum; 3, heating in oxygen. Activation energy $E_a = 0, 0.09; \blacktriangle, 0.09; \bullet, 0.08; \bullet, 0.03; \times, 0.03$ and $\triangle, 0.02$ eV.

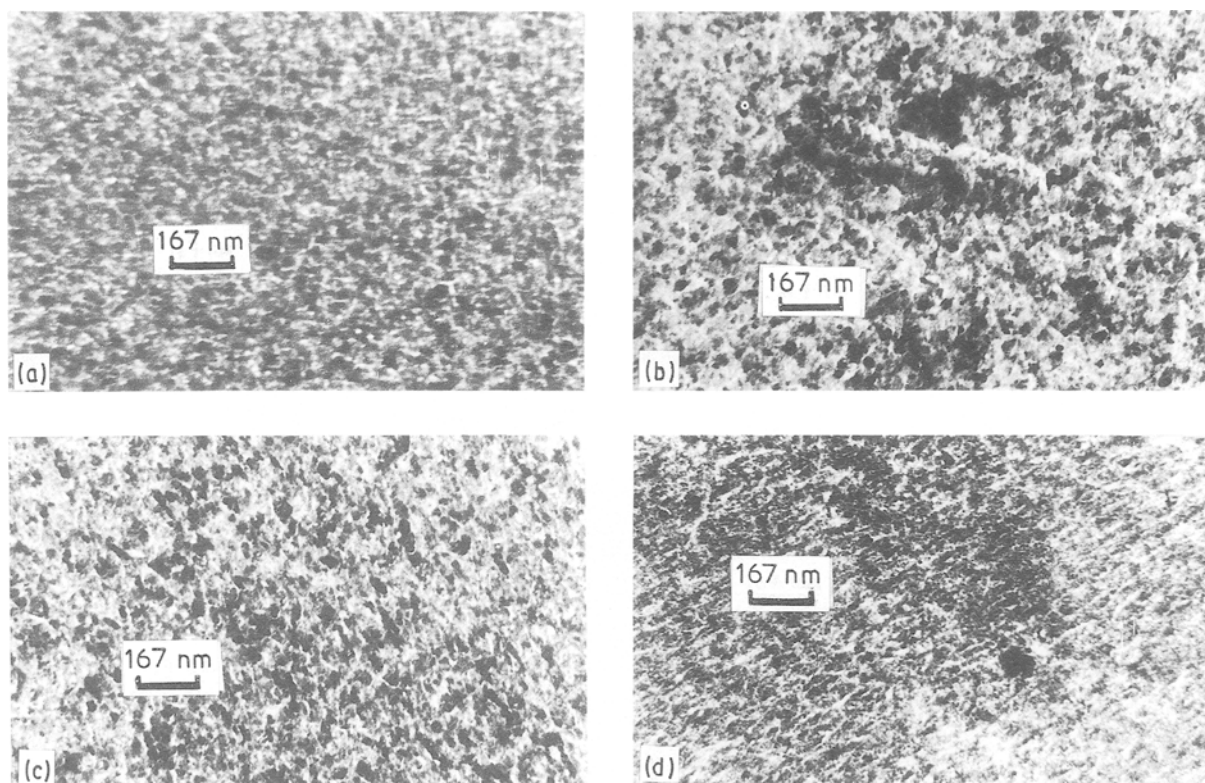


Figure 2 TEM micrographs for films with different treatments: (a) 80-nm thick, deposited at 1.3 nm s^{-1} , 300 K; (b) 140 nm, 1.3 nm s^{-1} , 300 K; (c) 80 nm, 1.3 nm s^{-1} , 375 K; (d) 80 nm, 3 nm s^{-1} , 300 K.

for an 80-nm thick film. The dashed lines 1–3 give similar heating and cooling curves, respectively, for a 100-nm thick film. In both cases, the films were deposited at 300 K at the same deposition rate (1.3 nm s^{-1}). Fig. 2a–d gives TEM micrographs of magnification $\times 60,000$ for an 80-nm thick film, and a 140-nm thick film, both deposited at 1.3 nm s^{-1} at 300 K, an 80 nm

thick film deposited at 375 K at 1.3 s^{-1} , and an 80-nm film deposited at 300 K at 30 nm s^{-1} respectively. Comparing Fig. 2a–d, it is observed that the grain size of the films increased with increasing film thickness and substrate temperature, and decreased with increasing deposition rate. The grain size of the 140-nm thick film is evidently larger than that of the 80-nm

film, both deposited at 300 K at 13 nm s^{-1} . But the slight improvement in crystallinity of the 80-nm film deposited at 375 K over that deposited at 300 K is not very evident from the figure. The decrease in grain size of the film deposited at 3.0 nm s^{-1} at 300 K compared to that deposited at 1.3 nm s^{-1} at 300 K is very clear from the two figures. Another point which should be mentioned is that the variation in grain size during the above thickness, substrate temperature and deposition rate ranges may not be appreciable.

Fig. 3 shows $\ln(R)$ against $1/T$ plotted for an 80-nm thick film deposited at two different substrate temperatures. Curves 1 and 2 in Fig. 3 represent the variation of film resistance with temperature in vacuum and oxygen, respectively, for the film deposited at 373 K. Curves 3 and 4 represent the similar variation in vacuum and oxygen, respectively, for the film deposited at 323 K.

Fig. 4 is the plot of $\ln(R)$ against $1/T$ for a film of thickness 80 nm deposited at two different deposition

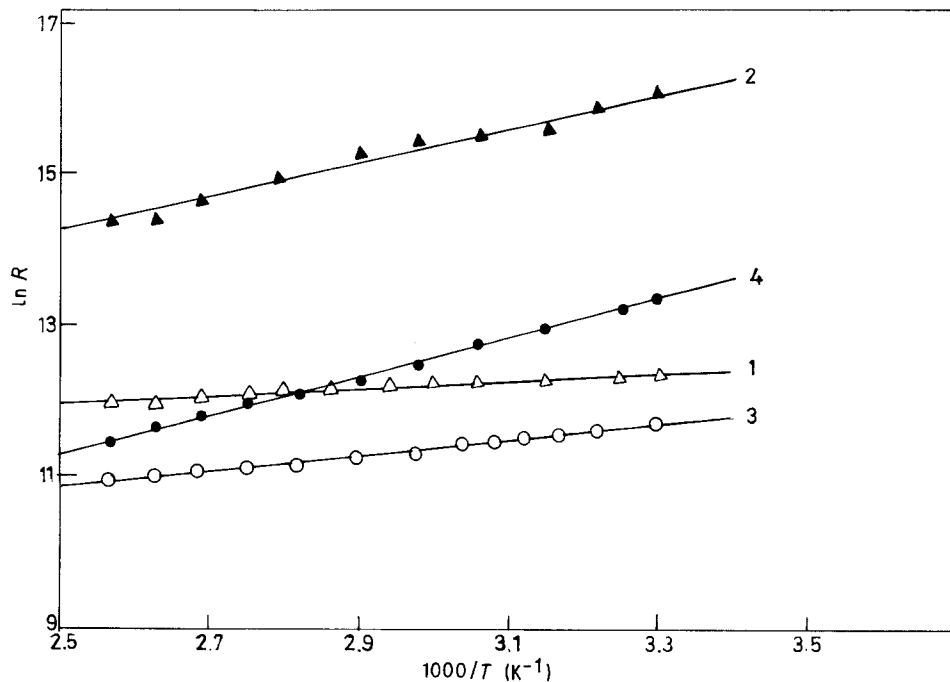


Figure 3 Effect of deposition temperature on film resistivity. $\ln(R)$ against $1/T$ plotted for a film of thickness 80 nm deposited at 373 K: 1, Cooling in vacuum; 2, heating in oxygen; and 323 K: 3, cooling in vacuum; 4, heating in oxygen. $E_a = \blacktriangle, 0.2; \bullet, 0.22; \triangle, 0.05; \circ, 0.1 \text{ eV}$.

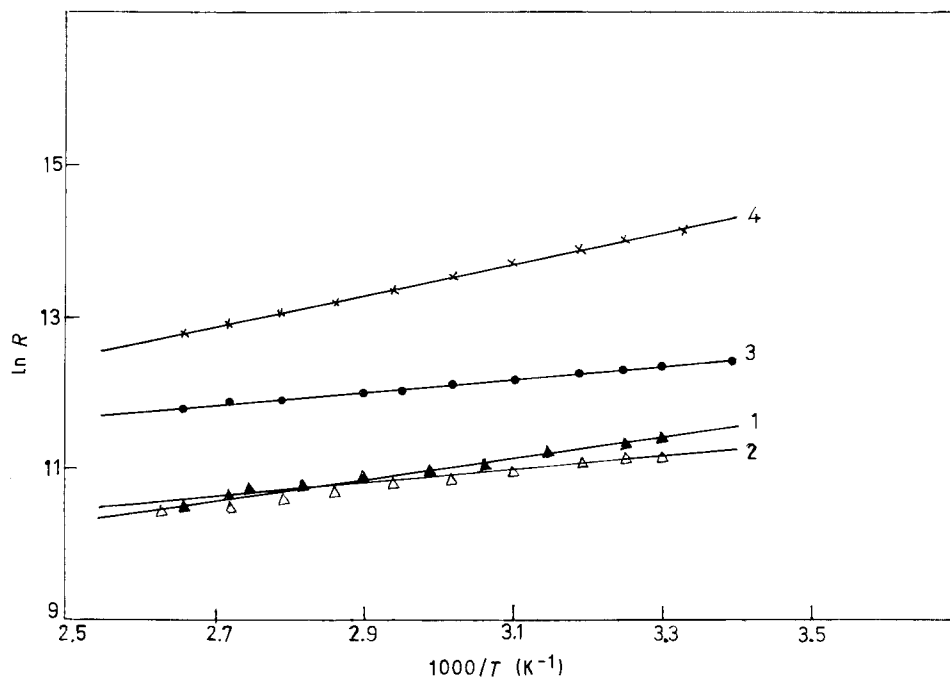


Figure 4 Effect of deposition rate on film resistivity. $\ln(R)$ against $1/T$ plotted for a film of thickness 80 nm deposited at a rate of 0.5 nm s^{-1} : 1, first heating in vacuum; 2, subsequent heating/cooling in vacuum; and 1.8 nm s^{-1} : 3, first heating in vacuum; 4, heating in oxygen. $E_a = \blacktriangle, 0.11; \triangle, 0.10; \bullet, 0.07; \times, 0.18 \text{ eV}$.

rates at 300 K. Curves 1 and 2 in Fig. 4 give the temperature variation of resistance during the first heating and subsequent cooling/heating in vacuum, respectively, for the film deposited at 0.5 nm s^{-1} . Curves 3 and 4 give the similar variation during the first heating in vacuum and the heating oxygen, respectively, for the film deposited at 1.8 nm s^{-1} .

Belyaev *et al.* [5–7] have studied the electrical conduction mechanism of $\text{CdSe}_x\text{Te}_{1-x}$ thin films. These films are inhomogeneous semiconductors with deep impurity levels possessing large values of potential relief inhomogeneity. At high temperatures ($> 300 \text{ K}$), the electrical conduction is effected by electrons excited from deep impurity levels to the percolation level, and is described by the relation [7]

$$\sigma = \sigma_0 \exp\left[-\frac{E_p - E_F}{kT}\right] \quad (1)$$

where E_p is the percolation level; E_F is the Fermi level; and σ is the electrical conductivity. As in the case of CdSe and CdTe, Seto's polycrystalline model [15] may be used to interpret the results.

$\text{CdSe}_{0.8}\text{Te}_{0.2}$ films have been found to behave more like CdSe than CdTe films. The ageing characteristics of these films are explained using an oxygen adsorption model [15, 16] which is also applicable to CdSe films [17–19]. Hence the observed experimental results for $\text{CdSe}_{0.8}\text{Te}_{0.2}$ films may be explained by taking into account the behaviour of CdSe films under similar circumstances.

Referring to Fig. 1, it is seen that the resistance of the 80-nm thick film is more than that of the 100-nm film in the temperature range 300–400 K. In both cases it was observed that the film resistance came to a low value after the first heating cycle in vacuum. Moreover, the conduction activation energy was also reduced after the first heating cycle in vacuum. But heating the film in oxygen resulted in an increase in activation energy. The electron micrographs (Fig. 2a and b) recorded an improvement in film crystallinity with increase in thickness. The reduction in film resistance with increasing film thickness may be explained by considering the improved crystallinity of thicker films, as intercrystalline potential barrier scattering [20, 21] is the major scattering mechanism in these films.

In CdSe films, three donor excitation levels of about 0.025, 0.14 and 0.4 eV have been observed by Snejdar and Jerho [22] and two levels of about 0.10 and 0.5 eV by Wagner and Breitweiser [19]. In CdTe films, we have observed a number of donor levels (both deep and shallow). Hence in $\text{CdSe}_{0.8}\text{Te}_{0.2}$, one may see a spectrum of conduction activation energies depending on the position of the donor levels. Dhere *et al.* [23] have observed that in CdSe films the amount of excess Cd increases with heat treatment. Because of the difference in vapour pressures, $\text{CdSe}_{0.8}\text{Te}_{0.2}$ will have a slight excess of Cd, which behaves as a donor impurity. The additional Cd excess formed by heat treatment may occupy shallow levels in the film, giving rise to reduced activation energy after the heat treatment in vacuum.

The increase in film resistance and conduction activation energy in the case of films heated in oxygen may be due to the total depletion of shallow donors by oxygen [18], as the films showed ageing when exposed to oxygen. Conductivity measurements showed that oxygen levels are at depths of about 0.20, 0.10 and 0.03 eV below the conduction band. This shows that oxygen depletes mainly the shallow impurity levels of the film.

Referring to Fig. 3, it is seen that the film deposited at higher substrate temperatures has greater resistance than that deposited at lower substrate temperatures.

The increase in film resistance of the film deposited at 373 K may be due to the increase in percentage Se of the film with increasing deposition temperature [22], which improves the film stoichiometry. As the deposition temperature increases, the condensation coefficients of the elements are modified in such a manner that the percentage Se in the film increases. Thus the amount of excess Cd donor impurity is reduced, resulting in increased film resistance. At high deposition temperatures, the donor impurities may form shallow levels because of the reduction in grain boundary width, hence the reduction in activation energy for films deposited at high substrate temperatures. The variation in grain size with increase in substrate temperature does not seem to have much effect on film resistance as compared to the increase in percentage Se in the film.

In this case depletion of shallow donors by oxygen may also be a reason for the increase in film resistance and conduction activation energy for the films heated in oxygen.

In Fig. 4, it is observed that films deposited at high deposition rates had higher resistance than those deposited at low deposition rates. This may be explained by the increase in percentage Te with increasing deposition rate [24]. Another factor which contributes towards the increase in film resistance with increase in deposition rate is the reduction in grain size with increasing deposition rate. Depletion of the film surface by oxygen atoms was seen again when the film was heated in oxygen (Fig. 4, curve 4). Table I gives the various activation energies observed for $\text{CdSe}_{0.8}\text{Te}_{0.2}$ films heated in vacuum and in oxygen. From a comparison of the above activation energies with those observed in CdSe and CdTe, it is seen that the activation energies of $\text{CdSe}_{0.8}\text{Te}_{0.2}$ fall at one of the values of CdSe or CdTe.

TABLE I Various activation energies (eV) observed in $\text{CdSe}_{0.8}\text{Te}_{0.2}$ films heated in vacuum and oxygen

Heated in vacuum	Heated in oxygen
0.025	0.03
0.03	0.10
0.10	0.20
0.14	–
0.20	–
0.35	–
0.40	–

4. Conclusions

CdSe_{0.8}Te_{0.2} thin films of various thicknesses, deposited at different rates and substrate temperatures and heat treated in vacuum and oxygen, showed the presence of both shallow and deep donor impurity levels. A spectrum of activation energies obtained which corresponded to these levels were found to fall at those values corresponding to either CdSe or CdTe. Films deposited at high deposition rates and substrate temperatures showed an increase in resistivity due to the increase in percentage Te and Se, respectively, in the films. The reduction in resistivity of the films heat treated in vacuum may be due to the increase in excess Cd in the films, which forms shallow donor levels. The fall in resistivity of the films with increasing film thickness is attributed to the improved crystallinity of the films, which confirms the fact that at high temperatures intercrystalline potential barrier scattering is the predominant scattering mechanism in these films. Films heated in oxygen showed an increase in resistivity, due to the depletion of the shallow donors by oxygen.

Acknowledgement

We wish to thank Professor K. Srinivasaraghavan of the Electron Microscopy Laboratory for TEM facilities.

References

1. T. H. WENG, *J. Electrochem. Soc.* **117** (1970) 725.
2. G. HODES, *Nature* **285** (1980) 29.
3. M. I. IZAKSON, N. YA. KARASIK, L. M. PRGKATOR, D. A. SAKESSEV, G. A. FEDOROVA and I. N. YAKIMENKO, *Inorg. Mater.* **15** (1979) 178.
4. S. UTHANNA and P. J. REDDY, *Solid State Commun.* **45** (1983) 979.
5. A. P. BELYAEV, I. P. KALINKIN and V. A. SANITAROV, *Sov. Phys. Semicond.* **17** (1983) 848.
6. *Idem.*, *ibid.* **18** (1984) 1234.
7. A. P. BELYAEV and I. P. KALINKIN, *Thin Solid Films* **158** (1988) 25.
8. I. D. BUDYONNAYA, A. M. PAVELETS, L. N. KHANAT and V. E. BADAN, *ibid.* **138** (1986) 163.
9. A. P. BELYAEV and I. P. KALINKIN, *Sov. Phys. Semicond.* **20** (1986) 1078.
10. A. P. BELYAEV, I. P. KALINKIN and V. S. SANITAROV, *ibid.* **19** (1984) 95.
11. V. A. SANITAROV, YU. K. EZHOVSKII and I. P. KALINKIN, *Inorg. Mater.* **13** (1977) 210.
12. I. B. SHAVEHENKO, YU. V. NIKOLSKII, E. M. SMIRNOVA, V. R. DARASHKEVICH and YU. E. SUTYRIN, *ibid.* **10** (1972) 184.
13. A. D. STUCKES and G. FARRELL, *J. Phys. Chem. Solids* **25** (1964) 77.
14. A. J. STRAUSS and J. STEININGER, *J. Electrochem. Soc.* **117** (1970) 1420.
15. J. Y. W. SETO, *J. Appl. Phys.* **46** (1975) 5247.
16. P. J. SEBASTIAN and V. SIVARAMAKRISHNAN, *ibid.* **65** (1989) 237.
17. *Idem.*, *Thin Solid Films* **189** (1990) 183.
18. G. A. SOMORJAI, *J. Phys. Chem. Solids* **24** (1963) 175.
19. R. G. WAGNER and G. C. BREITWEISER, *Solid State Electron.* **12** (1969) 229.
20. D. S. H. CHAN and A. E. HILL, *Thin Solid Films* **38** (1976) 163.
21. *Idem.*, *ibid.* **35** (1976) 337.
22. V. SNEJDAR and J. JERHOT, *ibid.* **11** (1972) 289.
23. N. G. DHERE, N. R. PARIKH and A. FERREIRA, *ibid.* **44** (1977) 83.
24. Y. KAWAI, Y. EMA and T. HAYASHI, *J. Appl. Phys.* **22** (1983) 803.

Received 10 September 1990
and accepted 28 February 1991